Trap-depth determination from residual gas collisions

J. Van Dongen,[1] C. Zhu,[1] D. Clement,[1] G. Dufour,[1] J. L. Booth,[2] and K. W. Madison[1,*]

[1]*Department of Physics & Astronomy, University of British Columbia, 6224 Agricultural Road, Vancouver, British Columbia, Canada V6T 1Z1*

[2]*Physics Department, British Columbia Institute of Technology, 3700 Willingdon Avenue, Burnaby, British Columbia, Canada V5G 3H2*

(Received 25 June 2010; published 16 August 2011)

We present a method for determining the depth of an atomic or molecular trap of any type. This method relies on a measurement of the trap loss rate induced by collisions with background gas particles. Given a fixed gas composition, the loss rate uniquely determines the trap depth. Because of the "soft" long-range nature of the van der Waals interaction, these collisions transfer kinetic energy to trapped particles across a broad range of energy scales, from room temperature to the microkelvin energy scale. The resulting loss rate therefore exhibits a significant variation over an enormous range of trap depths, making this technique a powerful diagnostic with a large dynamic range. We present trap depth measurements of a Rb magneto-optical trap using this method and a different technique that relies on measurements of loss rates during optical excitation of colliding atoms to a repulsive molecular state. The main advantage of the method presented here is its large dynamic range and applicability to traps of any type requiring only knowledge of the background gas density and the interaction potential between the trapped and background gas particles.

DOI: 10.1103/PhysRevA.84.022708 PACS number(s): 34.50.Cx, 37.10.Gh, 67.85.−d

I. MOTIVATION

The particle loss rate from a trap is one of the primary observables for probing the collisional physics of trapped gases. Measurements of trap loss are routinely made in a variety of experiments to deduce elastic and inelastic collision cross sections for intratrap collisions and for collisions between trapped species and externally introduced particles. Trap depth often plays an important role in the interpretation of these measurements. A well-studied example of this is the large intensity-dependent variation displayed by the two-body intratrap loss-rate coefficient for atoms trapped in a magneto-optical trap (MOT). This variation results from an interplay of trap depth and the energy imparted to trapped atoms due to hyperfine or fine structure changing collisions, as well as radiative escape [1–12]. More recently, inelastic and elastic collision rates in dipole traps have been of interest, particularly for metastable species [13,14]. The fraction of elastic collisions resulting in an evaporated atom depends on trap depth, which is a key parameter for evaporative cooling [13,15,16]. The lifetime dependence of a state-insenstive dipole trap on trap depth for cesium atoms has also recently been investigated [17]. Of course the most fundamental role of trap depth is that it be large enough to provide sufficient confinement, which has been an issue for experiments with buffer-gas-cooled atoms or molecules [18,19].

In recent years there has been interest in making precision determinations of collision cross-sections from measurements of particle loss rates due to externally introduced particles. These measurements involve collisions of trapped neutral particles with neutral atoms and molecules [20–24], electron beams [25–27], and trapped ions [28–30]. Photoionization cross sections have also been investigated though measurements of trap loss rates [31–33]. It has been shown for atoms exposed to background gas [34] and for molecules exposed to supersonic beams of atoms and molecules [23,24] that inelastic, and particularly elastic, collisional cross sections for trap loss vary significantly with trap depth. In these cases, the use of trap loss rates to determine with accuracy the cross sections for various processes, and to quantitatively compare measurement with theory, requires an accurate knowledge of the trap depth and an analysis of the energy transferred to the trapped target species. A useful corollary and the main result of this paper is that if the collision physics is well understood, measurement of the trap loss rate provides a way of accurately and reliably determining the trap depth.

For magnetic traps, the depth can be inferred from the trapping field geometry [35], set by rf frequency [36] or measured by Zeeman spectroscopy [37]. However, for dissipative traps that rely on radiation pressure forces, the trap depth is not easily estimated. Estimating the trap depth for a MOT from first principles requires the numerical integration of the optical Bloch equations for a multilevel atom [4–6,38,39] and often provides only qualitative agreement with experimental results. Trap depth measurement techniques for a MOT have been developed. For a MOT a kick-and-recapture method has been used [3,40]. The capture velocity for a beam-loaded MOT has been measured [41]. A method employing loss due to photoassociative excitation to a repulsive molecular potential has also been developed [42]. For trap depth determination of an optical dipole trap, measurements of beam waist and trap oscillation frequencies can be used to infer the depth. However, this procedure, as well as the interpretation of parametric heating experiments [43], can be complicated by the broadening and shift of the trap frequency and higher harmonics caused by the anharmonicity of the trapping potential [44–46]. A measurement of the differential ac Stark shift of the atoms in the dipole trap can provide a lower bound on trap depth so long as both the ground- and excited-state polarizabilites are well known. Pertinent to all trap depth calculations are the imperfections resulting from experimental realization. These imperfections include pointing stability, beam or field irregularities, interferences, and polarization

*madison@phas.ubc.ca

inhomogeneities. For these reasons, finding reliable methods to directly measure the trap depth in an experiment and to confirm existing methods is desirable and important.

In this paper we propose and demonstrate with an experiment that the depth of a trap can be determined from measurement of trap loss rate induced by collisions with a background gas. Our previous work [34] verified the shape of the predicted dependence of the collisional cross section for loss due to background collisions on trap depth in the region of trap depth attainable with our magnetic trap. In this work we provide further validation of this predicted dependence in the region of trap depth attainable with our MOT (from ∼0.5 to 3 K). For this validation at higher trap depths we used a trap-depth measurement technique based on photoassociative loss rates which we adapted and simplified from Hoffmann *et al*. [42]. Our work then also provides support of Hoffmann's work by showing the consistency of the trap depth predicted from loss rates and the trap depth as inferred from photoassociative loss rates.

The paper is organized as follows. In Sec. II we outline the proposed method. In Sec. III we review the theoretical calculation of collisional cross section. In Sec. IV we discuss experimental methods used to measure collisional cross section and to measure trap depth from photoassociative losses. In Sec. V we compare the trap depth of a MOT inferred from photoassociative losses to the trap depth inferred from particle loss rates induced by collisions with background gases. Section VI contains conclusions.

II. PROPOSAL

The particle loss rate due to collisions with a background vapor is the sum of loss rates induced by each of the species present in a vacuum,

$$\Gamma = \sum_i n_i \langle \sigma v \rangle_{X,i}, \tag{1}$$

where n_i is the density of the ith background species, X denotes the trapped species, and the velocity-averaged loss cross section $\langle \sigma v \rangle_{X,i}$ is a function of the trap depth U_{trap}. Because the terms $\langle \sigma v \rangle_{X,i}$ are all monotonically decreasing functions of U_{trap} [34], the loss rate Γ is a monotonically decreasing function of U_{trap}, and, for fixed background gas composition, the loss rate Γ *uniquely determines* U_{trap}. Because of the "soft," long-range nature of the van der Waals interaction, elastic collisions transfer kinetic energy to the trapped particles across a broad range of energy scales, from room temperature to the microkelvin energy scale. The resulting loss rate therefore exhibits variation over a large range of trap depths making this observable a powerful diagnostic with a large dynamic range.

The simplest approach to using the loss rate, Γ, to determine trap depth involves experimentally determining the dependence of Γ on U_{trap} in a particular vacuum environment using a trap of known but variable depth. Then the depth of any other confining potential of unknown depth in the same environment can be inferred from measurement of its background collision-induced loss rate. This approach does not require the addition of background gas other than what is present normally in steady state. An example would be determining the trap depth of an optical dipole trap by a comparison of its loss rate with the loss rate from a magnetic trap, whose depth can be tuned and known using radio frequency or microwave radiation. A caveat is that the loss cross section for certain background species may depend on the electronic state of the trapped species. Care must be taken, therefore, when characterizing the depth of a trap that contains trapped particles in both the ground and the excited electronic states.

There is an alternative *ab initio* approach to determining depth of a trap that does not rely on making heuristic measurements of loss rates from a trap of known depth. The approach is to measure the loss rate Γ as the density of a particular background species n_j is varied. The resulting loss-rate slope $\langle \sigma v \rangle_j$ *uniquely determines the trap depth* U_{trap}. The energy distribution imparted to the trapped species by collisions with species j can be computed from first principles using the interaction potentials, and the relationship between loss rate and trap depth can be computed. The computation is described in Ref. [34] and the fundamentals are repeated in the next section. Our proposed method involves using the measured value of loss-rate coefficient, $\langle \sigma v \rangle_j$, to give trap depth by inverting the calculated dependence of $\langle \sigma v \rangle_j$ on trap depth. This approach is based on well-established quantum scattering theory with no additional assumptions and is applicable to any atomic or molecular species and any type of trapping potential. This approach is also immune to any additional background trap loss due to species other than the one being introduced, no matter how significant. One caveat is the dependence of loss-rate coefficient, $\langle \sigma v \rangle_j$, on the state of the trapped species complicating computation of $\langle \sigma v \rangle_j$ for traps where a mixture of states (both ground and excited) is found, as in MOTs.

We perform this *ab initio* technique using a magnetic trap and a MOT for ^{87}Rb. To simplify the analysis, we introduce and vary the background gas density of ^{40}Ar. In this case, the only significant collisions that occur are elastic since Ar has no nuclear spin and, relevant to magnetic trapping, there is no collisional spin exchange. The cross section for spin-changing collisions arising from the spin-rotation interaction is expected to be exceedingly small [47,48]. In this regard, certain noble gas atoms are the species of choice. An additional advantage to the choice of ^{40}Ar in this case is that the long-range part of the interaction potential between Rb and Ar in their ground electronic states is similar to that when Rb is in its first excited state. For a collision between a ground-state Ar atom and a ground-state Rb atom ($5\,^2S_{1/2}$), $C_6 = 280.0 E_h a_B$ [49] compared to a collision between a ground-state Ar atom and a Rb atom in the excited ($5\,^2P_{1/2}$ or $5\,^2P_{3/2}$) electronic state where $C_6 = 924.1 E_h a_B\,(\Sigma)$ and $C_6 = 545.1 E_h a_B\,(\Pi)$ [50]. Here $E_h = 4.359\,739\,4(22) \times 10^{-18}$ J and a_B is the Bohr radius. This feature is important when dealing with a radiation pressure trap where some fraction of the trapped species will be found in the electronically excited state [51]. In this work, we compare the MOT trap depth as determined by trap loss measurements with a method based on photoassociation of atoms in a MOT with a blue-detuned laser [42,52].

III. THEORY

For completeness, we repeat a section from our previous work [34] describing the *ab initio* method to compute

the loss-rate slope $\langle \sigma v \rangle_{X,j}$ dependence on the trap depth $U_{\rm trap}$. When a room-temperature background vapor particle encounters a trapped atom, the collision energy is typically very high. Nevertheless, for elastic collisions with a large classical impact parameter, the momentum transferred and resulting scattering angle can be extremely small. Consequently, for a trap with finite depth, collisions below some critical scattering angle do not result in trap loss. The goal is therefore to compute the differential cross section and evaluate the fraction of collisions that occur above the critical scattering angle for loss.

Consider a trapped atom of velocity $\vec{v}_{\rm a}$ and mass $M_{\rm a}$ and a background particle of velocity $\vec{v}_{\rm b}$ and mass $M_{\rm b}$. The initial relative velocity is $\vec{v}_{\rm r} = \vec{v}_{\rm a} - \vec{v}_{\rm b}$, and momentum conservation requires that the change in these velocities is related by $\Delta\vec{v}_{\rm a} = \frac{\mu}{M_{\rm a}}\Delta\vec{v}_{\rm r}$, where the reduced mass is $\mu = \frac{M_{\rm a}M_{\rm b}}{M_{\rm a}+M_{\rm b}}$. Energy conservation requires that for elastic collisions $|\Delta\vec{v}_{\rm r}|^2 = 2|\vec{v}_{\rm r}|^2(1-\cos\theta)$, where θ is the collision angle between the initial ($\vec{v}_{\rm r}$) and final ($\vec{v}_{\rm r}{}'$) relative velocities. After the collision, the trapped atom kinetic energy will have changed by an amount $\Delta E = \frac{M_{\rm a}}{2}[(\vec{v}_{\rm a}+\Delta\vec{v}_{\rm a})^2 - \vec{v}_{\rm a}^2] = \frac{M_{\rm a}}{2}[2\vec{v}_{\rm a}\cdot\Delta\vec{v}_{\rm a} + |\Delta\vec{v}_{\rm a}|^2]$. If this change in kinetic energy exceeds the trap depth $U_{\rm trap}$, loss will occur. In the limit that the trapped particle has a negligible initial kinetic energy ($\vec{v}_{\rm a} \ll \Delta\vec{v}_{\rm a}$), we have that $\Delta E \simeq \frac{M_{\rm a}}{2}|\Delta\vec{v}_{\rm a}|^2$ and

$$\Delta E \simeq \frac{\mu^2}{M_{\rm a}}|\vec{v}_{\rm r}|^2(1-\cos\theta). \tag{2}$$

Therefore, trap loss will occur if the collision angle exceeds the minimum angle,

$$\theta_{\rm min} = \arccos\left(1 - \frac{M_{\rm a}U_{\rm trap}}{\mu^2|\vec{v}_{\rm r}|^2}\right). \tag{3}$$

The rate at which background particles are scattered from a single trapped atom into a solid angle $d\Omega$ is $n_{\rm b}|\vec{v}_{\rm r}|(d\sigma/d\Omega)d\Omega$, where $n_{\rm b}$ is the density of background particles and $(d\sigma/d\Omega)$ is the differential scattering cross section. Given this, we can estimate the loss rate from a trap of depth $U_{\rm trap}$ as

$$\gamma_{\rm loss} = n_{\rm b}v_{\rm prob}\sigma_{\rm loss} = n_{\rm b}v_{\rm prob}\int_{\theta_{\rm min}(v_{\rm prob})}^{\pi}(d\sigma/d\Omega)d\Omega, \tag{4}$$

where the relative collision velocity is assumed to be determined by the most probable velocity for the background particles, $|\vec{v}_{\rm r}| = v_{\rm prob}$. This loss rate is always smaller than the estimated total collision rate, $\gamma_{\rm C} = n_{\rm b}v_{\rm prob}\sigma$, since $\theta_{\rm min} > 0$. In the limit of a vanishingly small trap depth ($U_{\rm trap} \to 0$), the minimum collision angle approaches zero ($\theta_{\rm min} \to 0$) and *the loss rate equals the total collision rate*.

The differential cross section is equal to the square of the quantum-mechanical scattering amplitude, $d\sigma/d\Omega = |f(k,\theta)|^2$, and depends explicitly on the magnitude of the collision wave vector $k = \mu|\vec{v}_{\rm r}|/\hbar$. It is assumed that the interaction potential is central and therefore there is no azimuthal angular dependence. For a beam of incident scattering particles with wave number k, the cross section for loss-inducing collisions from a trap of depth $U_{\rm trap}$ is

$$\sigma_{\rm loss}(k) = \int_{\theta_{\rm min}(\hbar k/\mu)}^{\pi} 2\pi\,\sin\theta|f(k,\theta)|^2 d\theta. \tag{5}$$

To compute the loss rate induced by collisions with a background gas at temperature T, one must average over the Maxwell-Boltzman distribution of incident collision wave numbers. Assuming the trapped atom velocity is negligible, we have that $\vec{v}_{\rm r} \simeq \vec{v}_{\rm b}$ and $k = \mu|\vec{v}_{\rm b}|/\hbar$. The velocity averaged loss rate is $\langle\gamma_{\rm loss}\rangle = n_{\rm b}\langle v\sigma\rangle$, where

$$\langle v\sigma\rangle = \left(\frac{M_{\rm b}}{2\pi k_{\rm B}T}\right)^{3/2}\int_0^{\infty} 4\pi\,\sigma_{\rm loss}(k)\,v_{\rm b}^3 e^{-M_{\rm b}v_{\rm b}^2/2k_{\rm B}T}dv_{\rm b}. \tag{6}$$

In order to evaluate this expression, we need to determine the scattering amplitude, $f(k,\theta)$, given the interatomic potential between atoms a and b. The asymptotic form of the two-body scattering wave function is the sum of an incident plane wave and a scattered spherical wave [53] $\psi_k(\mathbf{r})|_{r\to\infty} = A(e^{ikz} + f(k,\theta)\frac{e^{ikr}}{r})$. Given a central potential, ψ and f can be expanded in terms of the Legendre polynomials,

$$\psi_k(r,\theta) = \sum_{l=0}^{\infty} R_l(k,r)P_l(\cos\theta), \tag{7}$$

$$f(k,\theta) = \sum_{l=0}^{\infty} f_l(k)P_l(\cos\theta). \tag{8}$$

This is an expansion into *partial waves* of angular momenta l. For sufficiently large r, the potential is negligible, and the radial functions must therefore asymptotically approach the form for a free particle,

$$R_l(k,r)|_{r\to\infty} = B_l\,j_l(kr) + C_l n_l(kr), \tag{9}$$

where j_l and n_l are the spherical Bessel and Neumann functions. The coefficients B_l and C_l can be written as $B_l = A_l\cos\delta_l$ and $C_l = -A_l\sin\delta_l$, where $A_l = (2l+1)i^l e^{i\delta_l}$ and where $\delta_l = \arctan(-C_l/B_l)$ is the *phase shift* of the lth partial wave [54,55]. These phase shifts also completely determine the scattering amplitude,

$$f(k,\theta) = \frac{1}{k}\sum_{l=0}^{\infty}(2l+1)e^{i\delta_l}\sin\delta_l P_l(\cos\theta). \tag{10}$$

The evaluation of the scattering amplitude and resultant collision cross section therefore requires finding the partial wave phase shifts, and this is done by numerical integration of the radial Schrödinger equation. We write the radial equation for the lth partial wave as

$$\left[\frac{d^2}{dr^2} + W_l(r)\right]\psi_l(r) = 0, \tag{11}$$

where

$$W_l(r) = k^2 - \frac{2\mu}{\hbar^2}V(r) - \frac{l(l+1)}{r^2}, \tag{12}$$

$$\psi_l(r) = kr\,R_l(r), \tag{13}$$

and $V(r)$ is the interatomic potential. The solution to the radial equation for each partial wave l is then independently computed using the log-derivative method [56]. The integration of the radial equation starts from a position deep inside the classically forbidden region and ends at a point in the asymptotic regime, beyond which the potential is essentially flat and the scattering phase shift is no longer changing. The

phase shift is found by matching this numerical solution in the asymptotic region to the asymptotic form [Eq. (9)] and by using $\frac{-C_l}{B_l} = \tan\delta_l$.

The resultant values for partial wave phase shifts δ_l depend on the incident wave vector magnitude $k = \mu|\vec{v}_r|/\hbar$. Given the results for a particular collision wave vector, the scattering amplitude can be constructed using Eq. (10) and inserted into Eq. (5) to compute the total cross section for loss-inducing collisions at that collision velocity. Repeating this procedure for a set of wave vectors chosen from a Maxwell-Boltzman distribution, the velocity-averaged rate of loss-inducing collisions from a background gas at temperature T [Eq. (6)] is evaluated. The velocity averaged rate of loss can be computed for a discrete set of trap depths and numerical fitting provides a functional form for the rate-loss dependence on trap depth applicable to a limited range of trap depth. This functional form can be inverted to provide a trap depth determination method from measured velocity-averaged rate of loss.

IV. EXPERIMENTAL METHODS

A. Residual gas collision experiment

The aim is to measure the particle loss rate due to background collisions, Γ, and to then infer the trap depth from the dependence of loss rate on the density of ^{40}Ar. The population dynamics in a trap can be modeled as

$$\frac{dN}{dt} = R - \Gamma N - \beta \int n^2(r,t) d^3r, \tag{14}$$

where N is the number of particles in the trap, R is the loading rate of particles into the trap, and Γ is the loss rate due to collisions between the trapped particles and the background gases. The final term depends on the density of particles in the trap, n, and accounts for particle loss arising from two-body inelastic collisions between trapped particles. These two-body inelastic collisions, characterized by β, include ground-state collisions and light assisted collisional losses present in a MOT (see, for example, [3–5,7,57,58] and references therein). Losses from three-body and higher-order intratrap collisions are assumed here to be negligible [7].

Our MOT, described in [59], collects and cools on the order of 10^6 rubidium atoms from a room-temperature Rb vapor of below 10^{-8} torr. The light for the MOT was provided by a laser system composed of grating-stabilized and injection-seeded diode lasers described previously [12,59]. After amplification, we have a maximum six-beam total power of 18.3 mW of pump or "cooling light" (driving transitions from $|F = 2\rangle \rightarrow |F' = 3\rangle$) and 0.3 mW of repump light (driving transitions from $|F = 1\rangle \rightarrow |F' = 2\rangle$) both operating on the $5\,^2S_{1/2} \rightarrow 5\,^2P_{3/2}$ transition. This light is combined and expanded to a $1/e^2$ horizontal (vertical) diameter of 7.0(9.5) mm, prepared with the correct polarization, and introduced into the MOT cell along the three mutually orthogonal axes in a retroreflection configuration. Our maximum total pump intensity is 34.5 mW cm^{-2}. We operate the MOT with an axial gradient of $b' = 27.9(0.3)$ G cm^{-1}. The anti-Helmholtz magnetic coils were used for both the MOT and for magnetic trapping of the rubidium atoms. Various pump detuning and intensities were used for our MOT to provide different trap depths for the MOT.

Previous work has shown that MOTs grow in number and density with a constant volume up to densities of 3×10^{10} cm^{-3}, where the outward pressure on the cloud from multiple scattering becomes significant [60]. For a constant volume MOT the density is modeled as $n(r,t) = n_0(t)e^{-(\frac{r}{a})^2}$, where $n_0(t)$ is the peak density of the MOT. In this regime the solution to Eq. (14) is

$$N(t) = N_{ss}\left(\frac{1 - e^{-\gamma t}}{1 + \xi e^{-\gamma t}}\right), \tag{15}$$

where $\gamma = \Gamma + 2\beta n_{ss}$ and $\xi = \frac{\beta n_{ss}}{\Gamma + \beta n_{ss}}$ [7,61–63]. In addition, this model predicts that the steady-state MOT number should follow,

$$N_{ss} = \frac{R}{\Gamma + \beta n_{ss}}, \tag{16}$$

where R is the loading rate of the MOT and n_{ss} is the average steady-state density of the MOT,

$$n_{ss} = \left(\frac{\int n^2\, d^3r}{\int n\, d^3r}\right)_{ss}. \tag{17}$$

In Eq. (17) the subscript ss refers to the integrals being performed for a steady-state MOT. For the MOT conditions used in these experiments, the two-body loss-rate coefficient, β, can range from 10^{-13} to 10^{-11} cm^3/s [2,6,12]. Higher β values have been found for MOTs with a larger magnetic field gradient and larger laser intensity [12]. With a steady-state MOT density on the order of 10^{10} cm^{-3}, the two-body loss rate, βn_{ss} ranges from 10^{-3} to 10^{-1} s^{-1}.

When ^{40}Ar is introduced to the sample volume the MOT losses are dominated by collisions between trapped atoms and the room-temperature argon atoms (i.e., $\Gamma > \beta n_{ss}$). Our measured MOT loss rates range from 0.5 to 2.0 s^{-1}, between 5 and 20 times the largest estimate for βn_{ss}. In addition, as the background argon pressure increases, the number of atoms in the MOT and the average steady-state density decrease, further reducing the relative significance of the two-body losses. In the limit where $\Gamma > \beta n_{ss}$, Eq. (15) can be replaced with

$$N(t) = \frac{R}{\Gamma}(1 - e^{-\Gamma t}). \tag{18}$$

The MOT filling data were fit to both models Eq. (15) and Eq. (18) and we found that model Eq. (18) provided the better fit. The results of fitting to Eq. (15) confirmed that for the MOT densities of this experiment, the two-body intratrap collision-induced loss rates were negligible in comparison with the losses arising from ^{87}Rb-^{40}Ar collisions.

When atoms are transferred from the MOT into the quadrupole magnetic trap (QMT) we find similarly that the atom number evolution in our MT is well described by

$$N(t) = N(0)e^{-\Gamma t}. \tag{19}$$

For a MT $R = 0$. In the absence of light the confining forces are much weaker, leading to an increase in trapping volume of around 10^4 times with a corresponding decrease in trapped-particle density so that the two-body inelastic losses can again be neglected.

Figure 1 shows an example of the atom number evolution in a MOT and a MT under the condition that the density-

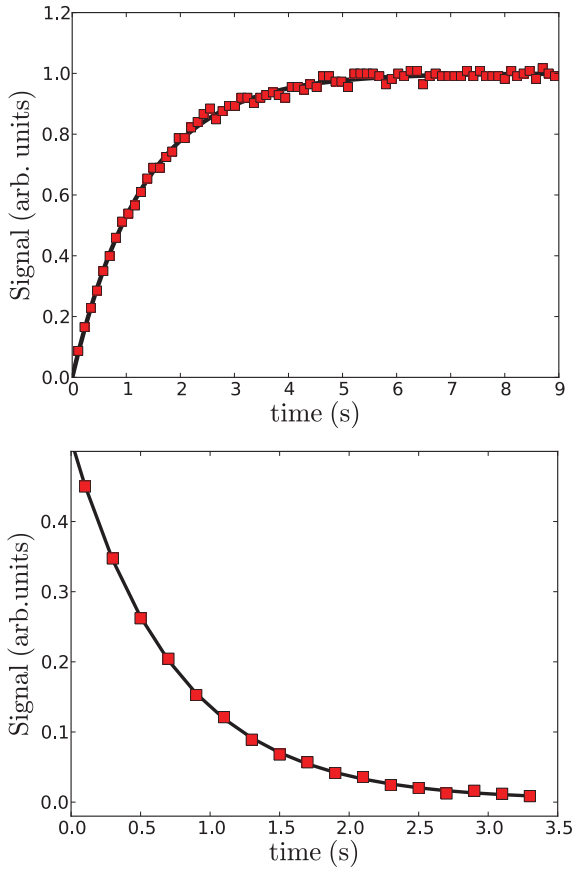

.

FIG. 1. (Color online) (a) Normalized ^{87}Rb MOT atom number as a function of time fit to Eq. (18). (b) Normalized ^{87}Rb atom number in a quadrupole magnetic trap as a function of time fit to the decay law given in Eq. (19).

dependent losses are negligible and Eqs. (18) and (19) are valid approximations. The loss rate Γ is extracted from a numerical fit of the data to these models. We have implicitly assumed here that the mean free path for collisions between the particles ejected from the trap and those that remain trapped is much larger than the trapped ensemble dimensions so that there are no secondary losses induced by these collisions. For large, dense ensembles this assumption may not be valid [64].

To circumvent the need to fully characterize the background gas composition, we isolate the loss of trapped particles due only to collisions with a specific species j by varying n_j and measuring the loss rate, Γ. Argon gas was introduced into the vacuum envelope through a leak valve attached to a pumping manifold as described in [34]. The loss rates of rubidium atoms from the MOT as a function of background argon pressure, under a variety of different trapping conditions (different "pump" intensities and detunings) were measured. The loss rates of atoms from a quadrupole magnetic trap (QMT) with a calculated depth of 3.14(0.84) mK were also measured at the same background argon pressures. As expected from Eq. (1), Γ varies linearly with a slope of $\langle\sigma v\rangle_{\mathrm{Rb},j}$, and this dependence is shown in Fig. 2.

The range of argon gas density explored in Fig. 2 corresponds to a pressure range from 1.8×10^{-8} to 6×10^{-8} torr. The argon pressure was measured using a residual gas analyzer

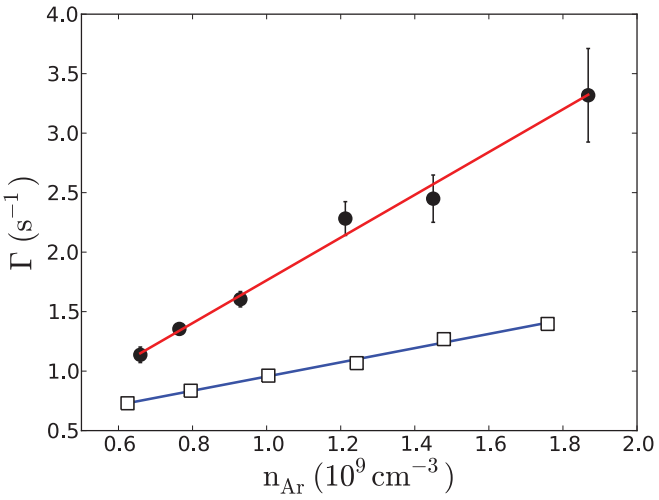

FIG. 2. (Color online) Total loss rate of trapped ^{87}Rb versus room-temperature argon gas density. The results are fit to a line and the slope provides the value of the velocity averaged collision rate $\langle\sigma v\rangle_{\mathrm{Rb,Ar}}$. The MOT (open squares) exhibits the smallest loss cross section due to a much larger effective trap depth ($\sim$2 K) than the MT (filled circles) where the $|F = 1, m_F = -1\rangle$ state was confined with a trap depth of 3 mK. The vertical error bars, most of which are smaller than the symbols, represent the statistical uncertainty in the loss rate based on fits similar to those shown in Fig. 1. The range of argon gas density here corresponds to a pressure range from 1.8×10^{-8} to 6×10^{-8} torr.

(RGA), which is generally subject to calibration drift over time and to calibration error that may introduce a systematic error to the measurement. To quantify and correct for systematic errors in the argon pressure (density) readings of the RGA, we measured the loss rate from a 3.14 (0.84)-mK-deep QMT for each of the different argon pressures used in these measurements. The actual density of argon at the position of the trap was then found by dividing this measured loss rate by the calculated loss-rate coefficient for this QMT. The Ar density as determined by the loss rate in the QMT differed from the density as measured by the RGA by at most 25%. This bootstrapping method coupled with collecting the data for different MOT trapping conditions at the same background argon pressure ensured that the relative uncertainty in the measured loss-rate coefficients was low.

The relationship between the collision loss-rate coefficient $\langle\sigma v\rangle_{\mathrm{Rb,Ar}}$ and the trap depth for elastic collisions between ^{40}Ar and trapped ^{87}Rb has previously been computed by us [34]. Figure 3 shows a plot of the predicted and experimentally determined trap depth as a function of the collision loss-rate coefficient, $\langle\sigma v\rangle_{\mathrm{Rb,Ar}}$. This figure constitutes the central result of this paper. As is intuitively clear, the deeper the trap, the lower the loss-rate coefficient. The trap depth can be experimentally determined by measuring the loss-rate coefficient and reading off the corresponding trap-depth value.

The theoretical prediction (solid line) was calculated using a Lennard Jones potential between the two species with a long-range van der Waals coefficient of $C_6 = 280.0\, E_h\, a_B^6$ [49,65,66]. The experimental data for trap depths $U_{\mathrm{trap}}/k_B <$ 10 mK taken from [34] were obtained with a QMT. The trap depth of the QMT is obtained from the gradient of

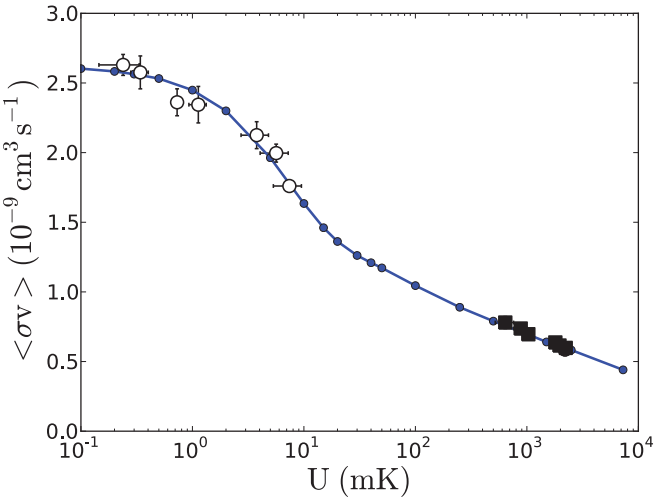

FIG. 3. (Color online) The experimentally measured (squares and open circles) and theoretically computed (solid circles) loss-rate constant $\langle \sigma v \rangle_{\mathrm{Rb,Ar}}$ versus trap depth for trapped ^{87}Rb atoms and room-temperature ^{40}Ar atoms. The line is only a guide for the eye. The data above 100 mK (squares) were obtained with a MOT while the data below 10 mK (open circles) were obtained with a quadrupole magnetic trap and are reproduced from [34]. Due to the difference in axial and radial magnetic field gradients, the MT depth limited by the vacuum cell walls is anisotropic. The resulting range of trap depths is indicated by the horizontal error bars on the MT data. The MOT depth was experimentally verified using an independent technique described in the text.

the quadrupole field and the physical size of the vacuum cell similar to that described in [67]. The magnetic coils here are external to the vacuum and the experimental cell (similar to that described in [59]) is square and only 1 cm wide. Atoms with sufficient energy could move from the center of the QMT to the cell wall where they would contact it, thermalize, and thus be lost from the trap. Due to the factor of two difference in axial and radial magnetic field gradients (as well as the effect of gravity), the QMT depth as limited by the walls is anisotropic. The resulting range of trap depths is indicated by the horizontal error bars on the QMT data in Fig. 3. The data for trap depths $U_{\mathrm{trap}}/k_{\mathrm{B}} >$ 100 mK were obtained with a MOT operating under different pump detunings and intensities, and the trap depth was measured in each case using the photo-association technique pioneered by Walker's group [42,52]. The details of this measurement are described below. The maximum MT depth that could be achieved in our experiment was limited to 10 mK set by the maximum field gradient we could produce with our quadrupole coil pair, while the minimum trap depth we could work with for the MOT (600 mK) was limited by the signal to noise of our atom detection scheme. MOT depths as low as 200 mK have been achieved using large magnetic field gradients [57].

B. MOT depth measurement from photoassociation

As a verification of our proposed technique for measurements of the MOT depth, an independent trap-depth measurement was performed using the technique described by Hoffmann *et al.* [42]. In this scheme, an additional tunable laser (referred to as a catalysis laser) is focused onto the MOT. For our experiment the intensity was $\sim$2 W/cm^2. Its frequency is chosen to be close to but above (typically by a few GHz) the atomic resonance (in this case, the $5\,^2S_{1/2} \rightarrow 5\,^2P_{3/2}$ transition in ^{87}Rb) by an amount Δ. Since atoms in the MOT are predominantly in the upper hyperfine ground state, the detuning reported here is measured with respect to the $F = 2 \rightarrow F' = 3$ transition. When two colliding Rb atoms within the MOT approach each other, they can resonantly absorb a photon from the catalysis laser field which excites them to a dissociative molecular state with an energy of $h\Delta$ above threshold [68,69]. The molecule then dissociates in a time much less than the excited-state lifetime, and the two atoms fly apart with equal and opposite momenta in the center-of-mass frame, each acquiring a kinetic energy of $E_{\mathrm{cl}} = \frac{h\Delta}{2}$. If this kinetic energy is small compared to the trap depth, the atoms will remain in the MOT and will be cooled again. However, when the acquired kinetic energy approaches the MOT depth ($h\Delta \simeq 2U_{\mathrm{trap}}$), the atoms will escape with high probability and trap loss will be observed. Since a MOT includes both conservative and dissipative forces, the trap depth of the MOT is defined as the kinetic energy associated with a particle moving at the escape velocity. The aim of this technique, therefore, is to determine the trap loss probability dependence on the energy E_{cl}.

The population dynamics in the trap including the two-body inelastic loss induced by the catalysis laser can be modeled as

$$\frac{dN}{dt} = R - \Gamma N - (\beta + d \cdot \beta_{\mathrm{cl}}) \int n^2(r,t) d^3r, \qquad (20)$$

where β_{cl} is the loss-rate coefficient for photoassociative collisions induced by the catalysis laser, and d is the duty factor of the catalysis laser. Following the treatment given in Ref. [42], we note that the term $\beta_{\mathrm{cl}} \propto P(E_{\mathrm{cl}})\sigma_{\mathrm{cl}}$, where $P(E_{\mathrm{cl}})$ is the trap loss probability at energy E_{cl} and σ_{cl} is the cross section for the photoassociative collision. At low total pump laser intensity, $\sigma_{\mathrm{cl}} = \pi r_{\mathrm{C}}^2 f$, where r_{C} (the "Condon radius") is the interatomic separation at which the laser is resonant with the energy of the dissociative molecular state. Given the interaction potential energy above threshold is $V(R)$, r_{C} is defined by $V(r_{\mathrm{C}}) = h\Delta$. The factor f is the excitation probability and is proportional to the resonant interaction time. Since the interaction time is inversely proportional to the slope of the potential dV/dR at r_{C}, we can write $\sigma_{\mathrm{cl}} \propto R^2(dV/dR)^{-1}|_{R=r_{\mathrm{C}}}$. In the case of ^{87}Rb-^{87}Rb* collisions, the resonant dipole-dipole interaction is of the form $V(R) \sim R^{-3}$, and so $\sigma_{\mathrm{cl}} \propto \Delta^{-2}$ [52,70]. We find, therefore, that the loss-rate coefficient $\beta_{\mathrm{cl}} \propto P(E_{\mathrm{cl}})/\Delta^2$ should theoretically remain small for $E_{\mathrm{cl}} < U_{\mathrm{trap}}$, exhibit a sharp rise to a maximum when $E_{\mathrm{cl}} = U_{\mathrm{trap}}$, and decrease as the detuning is increased beyond this point. Since the MOT depth may be anisotropic and since there are two ground states (in the case of ^{87}Rb, separated by 6.8 GHz) from which the Rb atoms can be excited, the probability of loss $P(E_{\mathrm{cl}})$ will not be a perfect step function equal to 1 when $h\Delta = 2U_{\mathrm{trap}}$. Nevertheless, we still expect the peak in the catalysis laser-induced loss rate to occur at or near the value of the detuning corresponding to the depth of the trap or, more precisely, the effective escape kinetic energy of

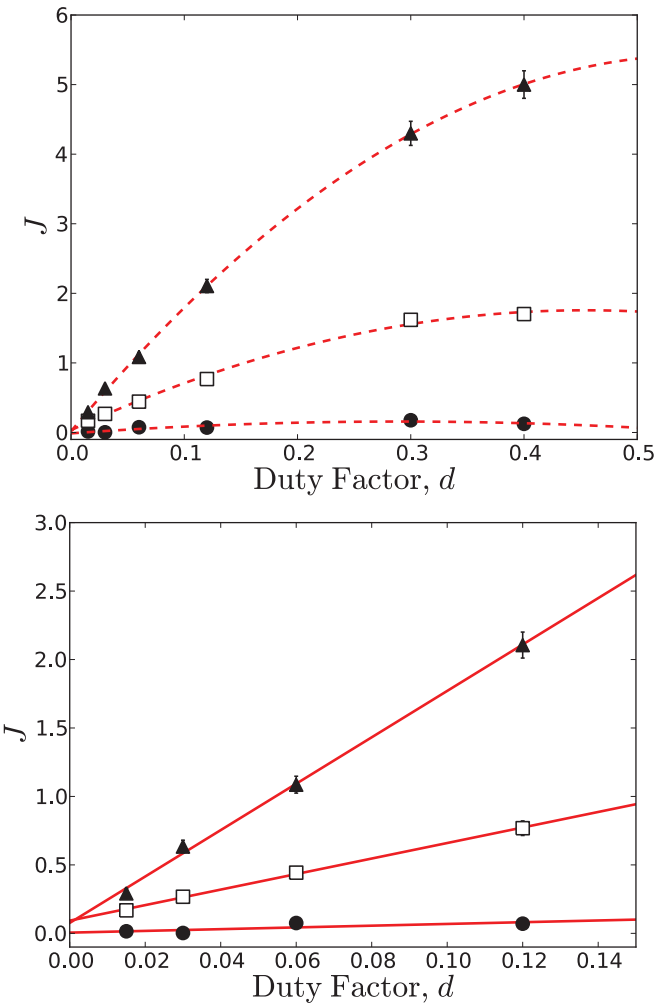

FIG. 4. (Color online) $J = \frac{N_{ss}^0}{N_{ss}} - 1$ as a function of the duty factor d for three different catalysis laser detunings $\Delta_1 = 27.3$ GHz (solid triangles), $\Delta_2 = 16.2$ GHz (open squares), and $\Delta_3 = 5.7$ GHz (solid circles) with a MOT pump detuning of -5 MHz and pump intensity of 2.7 mW/cm^2. $\frac{N_{ss}^0}{N_{ss}}$ is the ratio of the steady-state number with the catalysis laser off to the number with the laser on. The dotted lines are guides for the eye, while the solid lines are linear fits to the data excluding the points at large d where the variation is nonlinear. The slope of this ratio versus d is equal to $\frac{\beta_{cl} n_{ss}}{(\Gamma+\beta n_{ss})}$ and is proportional to the catalysis laser-induced loss rate, β_{cl}.

atoms from the MOT. The aim, therefore, is to determine the catalysis laser-induced loss rate, β_{cl}, as a function of Δ.

Equation (20) can be solved for the steady-state trap population

$$N_{ss} = \frac{R}{\Gamma + (\beta + d\beta_{cl}) n_{ss}}, \tag{21}$$

where n_{ss} is the average steady-state density distribution of the trapped atoms. The loss rate per atom due to the catalysis laser-induced photoassociation is $\beta_{cl} n_{ss} d$. If this loss rate is too significant, the MOT atom number can reduce to the point where n_{ss} is suppressed with respect to its value when the catalysis laser is off, and this variation can complicate the interpretation. Hoffmann *et al.* limited the density variation induced by the catalysis laser while ensuring that the instantaneous intensity was always the same by turning on and off the laser with a variable duty factor, $d \in [0,1]$. This was done, instead of simply lowering the intensity of the catalysis laser, to avoid additional complications arising from the nontrivial intensity dependence of the photoassociation process [52]. The duty factor was controlled via feedback to maintain a constant steady-state atom number and density in the MOT as the catalysis laser detuning was varied. The loss-rate coefficient, β_{cl}, was, then, proportional to the inverse of the duty factor.

In our experiment we have simplified this approach by recording the steady-state MOT number at each catalysis laser detuning for a range of duty factors, N_{ss}, and we compare these to the steady-state MOT number in the absence of the catalysis laser, N_{ss}^0. The ratio of these two steady-state signals is

$$\frac{N_{ss}^0}{N_{ss}} = 1 + \frac{\beta_{cl} n_{ss} d}{\Gamma + \beta n_{ss}}. \tag{22}$$

From Eq. (22) we define the parameter,

$$J = \frac{N_{ss}^0}{N_{ss}} - 1 = \left(\frac{\beta_{cl} n_{ss}}{\Gamma + \beta n_{ss}} \right) d. \tag{23}$$

A plot of J as a function of the duty factor is linearly proportional to β_{cl} provided the steady-state density is constant. When this assumption breaks down, namely when the duty factor is high, the variation of J with d is no longer strictly linear. Figure 4 shows this ratio for various values of d at different values of the detuning Δ and for a MOT with a cooling laser detuning of -5 MHz and a total pump laser intensity of 2.7 mW/cm^2. In the range of small d, where the dependence is linear, we extract the slopes which are proportional to the catalysis laser-induced loss rate and plot them as a function of detuning Δ in Fig. 5. The peak loss rate for the data shown occurred at 27(5) GHz, corresponding to an effective trap depth of 0.64(0.12) K.

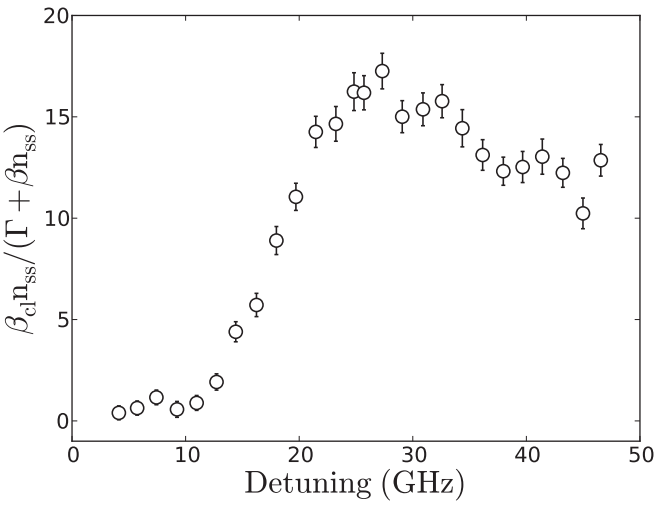

FIG. 5. The quantity $\frac{\beta_{cl} n_{ss}}{\Gamma + \beta n_{ss}}$, proportional to the photoassociation induced loss rate, measured as a function of the catalysis laser detuning, Δ. These data correspond to a MOT with a cooling laser detuning of -5 MHz and a total pump laser intensity of 2.7 mW/cm^2 (corresponding to a total power of 1.4 mW for the MOT). The peak loss rate occurred at 27(5) GHz and indicates that the effective trap depth was 0.64(0.12) K.

V. RESULTS AND DISCUSSION

Table I lists the observed loss-rate coefficients $\langle \sigma v \rangle_{\mathrm{Rb,Ar}}$ for different MOT pump detunings and intensities. For trap depths in the range from 0.5 K to 3.0 K, we have approximated the model loss-rate coefficient by

$$\langle \sigma v \rangle = [0.702 - 0.132\ \ln(U_{\mathrm{trap}}/1\,\mathrm{mK})] \times 10^{-9}\ \mathrm{cm}^3\,\mathrm{s}^{-1}. \tag{24}$$

This approximation is a fit to calculated values of $\langle \sigma v \rangle_{\mathrm{Rb,Ar}}$ at discrete trap depths. The effective MOT depth is deduced for each value of $\langle \sigma v \rangle$ by inverting Eq. (24) and solving for U_{trap}. The results, compared to the trap depths deduced via the catalysis laser measurements are summarized in Table II. Figure 6 shows a plot of the measured loss-rate coefficient as a function of the MOT depth deduced from the catalysis laser photoassociation. Overlaid on these data is the model elastic collision loss-rate coefficient (solid curve). The close agreement between the data and the prediction indicates that the trap depth as determined by the loss rate is consistent with the depth as determined by the catalysis laser method. Figure 7 displays the same results in a different format. Here the MOT depths deduced from the collision loss-rate coefficient are plotted versus the depths measured by the catalysis laser method. The uncertainties in the measurements translate into a range of trap depths. These values are plotted as a function of the effective MOT depths deduced using the catalysis laser technique. The solid line indicates ideal agreement and, as is seen, the two methods agree within our measurement error.

The loss-rate method for determining trap depth has several advantages. It is a simpler to implement than the catalysis laser technique. Trap loss, deduced from a MOT loading curve or from population decay from a magnetic (or optical dipole) trap is readily measured. By contrast, the catalysis technique requires the use of an additional, widely tunable laser which must be carefully controlled to ensure that the trap density is not significantly perturbed. As the total pump laser intensity increases, the two-body loss rate of atoms from the MOT increases, increasing $\Gamma + \beta n_{\mathrm{ss}}$ and reducing the relative size of the peak in $\frac{\beta_{\mathrm{cl}} n_{\mathrm{ss}}}{\Gamma + \beta n_{\mathrm{ss}}}$ as a function of catalysis laser detuning (see Fig. 8). This leads to larger uncertainty in the trap depth determination using the photoassociation technique. The catalysis method also suffers from the complication of having several nondegenerate ground states and several repulsive states that are excited by the catalysis laser, leading to a broadening of the peak loss rate versus detuning. This and a nontrivial intensity dependence on the photoassociation rate can complicate the trap depth determination [52]. Moreover, we note that the photoassociative method relies on intratrap collisions between particles in a known internal state and is therefore not useful if the trap density is too low or if the trapped ensemble includes particles in different internal states with significantly different excitation energies.

Finally, some complications of determining the MOT trap depth from trap loss measurements should be pointed out. In the MOT a fraction of the trapped atoms are in an excited electronic state ($^2P_{3/2}$). The collision rate between a background gas atom or molecule and atoms in the trap will depend on the collision partners and the electronic state of the trapped atoms. The analysis presented in this paper has assumed that the majority of the atoms in the MOT are in the ground electronic state and that the long-range interaction potential can be characterized by a single van der Waals C_6 coefficient. If a sufficient fraction of the atoms are in an excited electronic state, then one would expect to observe deviations from the ground-state prediction presented here since the C_6 coefficient for ^{87}Rb and ^{40}Ar depends on the electronic state

TABLE I. Measured loss-rate coefficients $\langle \sigma v \rangle_{\mathrm{Rb,Ar}}$ from the MOTs under different trapping conditions. The intensity is the total pump intensity for the six-beam MOT.

MOT detuning (MHz)	Intensity (mW cm^{-2})	Loss-rate coefficient ($\times 10^{-9}$ cm^3 s^{-1})
−5	2.7	0.780 (0.043)
−8	2.7	0.737 (0.033)
−10	2.7	0.696 (0.031)
−12	6.9	0.637 (0.008)
−12	9.6	0.615 (0.006)
−12	34.5	0.598 (0.003)

TABLE II. Measured effective trap depth for a ^{87}Rb MOT based on loss-rate coefficient measurements ($U_{\langle \sigma v \rangle}$) and on catalysis laser photoassociation losses (U_{cl}). The intensity is the total pump intensity for the six-beam MOT.

Detuning (MHz)	Intensity (mW cm^{-2})	$U_{\langle \sigma v \rangle}$ (K)	U_{cl} (K)
−5	2.7	0.55 (0.15)	0.64 (0.12)
−8	2.7	0.77 (0.17)	0.88 (0.12)
−10	2.7	1.05 (0.22)	1.03 (0.12)
−12	6.9	1.64 (0.10)	1.80 (0.18)
−12	9.6	1.93 (0.07)	1.99 (0.18)
−12	34.5	2.20 (0.05)	2.23 (0.24)

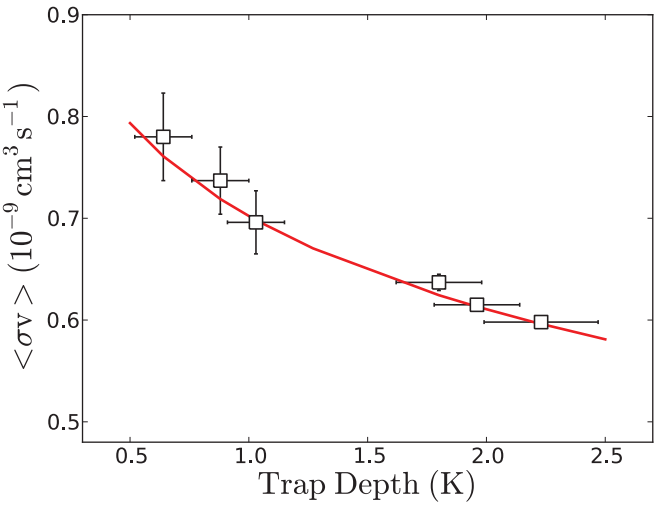

FIG. 6. (Color online) The open squares are the measured trap loss coefficients plotted at the trap depths deduced by the catalysis laser technique. The solid curve is the model trap loss-rate coefficient as a function of trap depth. The agreement between the data and the model indicate that the trap depth can be deduced from a measurement of the loss-rate coefficient.

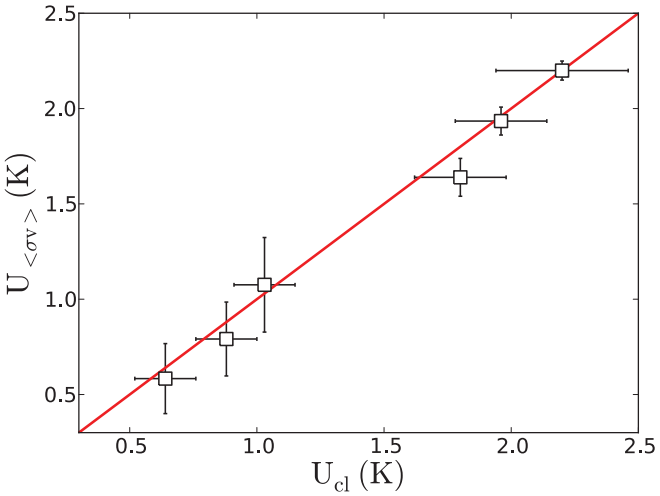

FIG. 7. (Color online) The measured MOT trap depths using the trap loss method, $U_{\langle\sigma v\rangle}$, versus the depth determined by the catalysis laser method, U_{CL}. The line indicates the locus of values corresponding to hypothetically perfect agreement. As is evident, the two techniques yield the same results within measurement error.

of ^{87}Rb. To quantify the effect of excited-state collisions we compute the excited-state fraction, f, using a simple two-level model with a correction for the saturation intensity as described in [51]. From the expected dispersion coefficients for interactions between ^{87}Rb in the $^2P_{3/2}$ state and ^{40}Ar in its ground electronic state [50], we estimate that deviations from the predicted loss-rate coefficients presented would be less than 10% for all MOT settings studied, within the uncertainty of the current measurements. This estimate is based on the

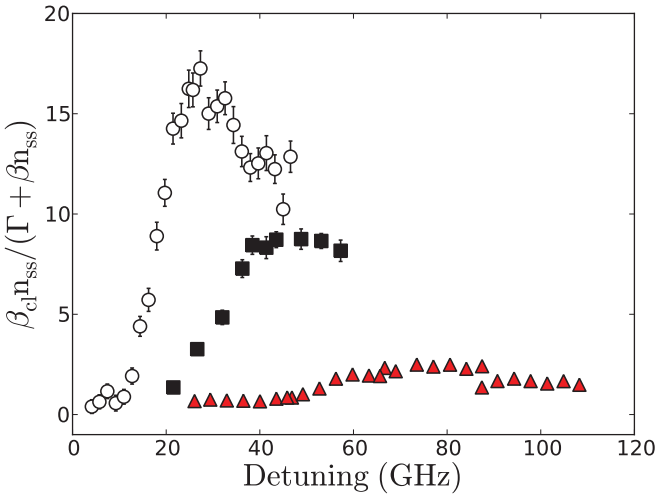

FIG. 8. (Color online) Catalysis laser data for MOTs with pump laser settings of −5 MHz 2.7 mW/cm^2 (circles), −10 MHz 2.7 mW/cm^2 (squares), and −12 MHz 9.6 mW/cm ^{2} (triangles), corresponding to measured trap depths of 0.64 (0.12) K, 1.03 (0.12) K, and 1.99 (0.18) K, respectively. As the trap depth increases, and/or the photoassisted two-body losses induced by the MOT pump laser increase, the less sensitive is the catalysis laser trap depth measurement.

assumption that the loss-rate coefficient measured, $\langle\sigma v\rangle_{\mathrm{meas}}$, can be expressed in terms of the loss-rate coefficients from collisions of ^{40}Ar with trapped ^{87}Rb in its ground state, $\langle\sigma v\rangle_{\mathrm{g}}$, and its excited state, $\langle\sigma v\rangle_{\mathrm{e}}$, as

$$\langle\sigma v\rangle_{\mathrm{meas}} = f\langle\sigma v\rangle_{\mathrm{e}} + (1-f)\langle\sigma v\rangle_{\mathrm{g}}. \tag{25}$$

Higher-precision measurements, measurements on MOTs with a higher fraction of excited state atoms, or loss-rate measurements of rubidium atoms due to collisions with hot rubidium atoms (where the long range Rb-Rb* interaction is dominated by a $1/R^3$ dependence) would provide a method of precisely measuring the excited-state fraction in a MOT.

Our proposed trap depth determination method depends on measurements of density of an introduced species. A bootstrap method for correcting for systematic deviations in pressure measurements was described in Sec. IV, which relied upon the presence of an additional type of trap whose depth could be known more readily. In our case we used the measurement of the loss rate from a 3.14 (0.84)-mK-deep QMT to quantify and correct for systematic errors in the argon pressure readings from the RGA. Without the bootstrap correction, the trap loss technique of inferring trap depth from measurement of loss-rate coefficient remains valuable but its accuracy will be subject to the accuracy at which the density of the introduced background gas species (Ar in our case) can be measured.

Finally, we note that this method is most accurate for regions where the loss-rate coefficient, $\langle\sigma v\rangle$, changes the most rapidly with trap depth which corresponds to trap depths on the order of the energy scale for quantum diffractive collisions, $\epsilon_{\mathrm{d}} = 4\pi\hbar^2/m\sigma$, where m is the trapped atom mass and σ is the total collision cross section between the trapped particle and the background particle [34,71]. For Ar-Rb collisions, this energy scale is approximately 10 mK, and a trap of this depth would exhibit roughly half the loss rate of a trap with vanishingly small depth. With the proper choice of a different background gas with a larger (smaller) total cross section, this energy scale of maximum sensitivity can be conveniently shifted to lower (higher) values.

VI. CONCLUSIONS

In summary, a technique for measuring the depth of any type of trap based on particle loss-rate measurements induced by elastic collisions with a background gas is presented. This technique is demonstrated with the use of trapped, laser-cooled rubidium atoms to measure the trap depth of a MOT based on the cross section for ^{87}Rb-^{40}Ar collisions. The trap depth is extracted by comparing the measured elastic collision loss-rate coefficients over the range of 0.5 K to 2.5 K to the values predicted using the known long-range C_6 coefficient. The trap depth results obtained from this method are verified by trap depth measurements based on trap loss induced with a catalysis laser. The two techniques agree within experimental uncertainties. An advantage offered by the collision loss-rate measurement is its simplicity of implementation. The trap loss technique for a MOT has a convenient bootstrap in that one can eliminate systematic errors introduced by inaccurate pressure measurements by comparing the loss-rate coefficient from a

trap of known depth (for example, a QMT) to that of the MOT. The trap loss technique is applicable to any type of trap, including an optical or a QMT, and at extremely low densities where intratrap collisions are rare. When used for a MOT, the loss rate will be sensitive to the presence of excited-state atom collisions (for example, Rb-Rb*) and may provide a method for sensitively measuring the excited-state fraction in the MOT.

ACKNOWLEDGMENTS

The authors acknowledge the support of the Canadian Institute for Advanced Research (CIfAR), the Natural Sciences and Engineering Research Council of Canada (NSERC), the Canadian Foundation for Innovation (CFI), the Peter Wall Institute for Advanced Studies, and the BCIT School of Computing and Academic Studies Professional Development Fund.

[1] D. Sesko, T. Walker, C. Monroe, A. Gallagher, and C. Wieman, Phys. Rev. Lett. **63**, 961 (1989).
[2] C. D. Wallace, T. P. Dinneen, K.-Y. N. Tan, T. T. Grove, and P. L. Gould, Phys. Rev. Lett. **69**, 897 (1992).
[3] J. Kawanaka, K. Shimizu, H. Takuma, and F. Shimizu, Phys. Rev. A **48**, R883 (1993).
[4] N. W. M. Ritchie, E. R. I. Abraham, and R. G. Hulet, Laser Phys. **4**, 1066 (1994).
[5] N. W. M. Ritchie, E. R. I. Abraham, Y. Y. Xiao, C. C. Bradley, R. G. Hulet, and P. S. Julienne, Phys. Rev. A **51**, R890 (1995).
[6] S. D. Gensemer, V. Sanchez-Villicana, K. Y. N. Tan, T. T. Grove, and P. L. Gould, Phys. Rev. A **56**, 4055 (1997).
[7] J. Weiner, V. S. Bagnato, S. Zilio, and P. S. Julienne, Rev. Mod. Phys. **71**, 1 (1999).
[8] G. D. Telles, W. Garcia, L. G. Marcassa, V. S. Bagnato, D. Ciampini, M. Fazzi, J. H. Müller, D. Wilkowski, and E. Arimondo, Phys. Rev. A **63**, 033406 (2001).
[9] A. R. L. Caires, G. D. Telles, M. W. Mancini, L. G. Marcassa, V. S. Bagnato, D. Wilkowski, and R. Kaiser, Braz. J. Phys. **34**, 1504 (2004).
[10] B. Ueberholz, S. Kuhr, D. Frese, V. Gomer, and D. Meschede, J. Phys. B **35**, 4899 (2002).
[11] G. Auböck, C. Binder, L. Holler, V. Wippel, K. Rumpf, J. Szczepkowski, W. E. Ernst, and L. Windholz, J. Phys. B **39**, S871 (2006).
[12] K. Ladouceur, B. G. Klappauf, J. Van Dongen, N. Rauhut, B. Schuster, A. K. Mills, D. J. Jones, and K. W. Madison, J. Opt. Soc. Am. B **26**, 210 (2009).
[13] A. Traverso, R. Chakraborty, Y. N. Martinez de Escobar, P. G. Mickelson, S. B. Nagel, M. Yan, and T. C. Killian, Phys. Rev. A **79**, 060702 (2009).
[14] A. Yamaguchi, S. Uetake, D. Hashimoto, J. M. Doyle, and Y. Takahashi, Phys. Rev. Lett. **101**, 233002 (2008).
[15] R. Chicireanu, Q. Beaufils, A. Pouderous, B. Laburthe-Tolra, E. Maréchal, J. V. Porto, L. Vernac, J. C. Keller, and O. Gorceix, Phys. Rev. A **76**, 023406 (2007).
[16] R. deCarvalho and J. Doyle, Phys. Rev. A **70**, 053409 (2004).
[17] P. Phoonthong, P. Douglas, A. Wickenbrock, and F. Renzoni, Phys. Rev. A **82**, 013406 (2010).
[18] J. G. E. Harris, R. A. Michniak, S. V. Nguyen, W. C. Campbell, D. Egorov, S. E. Maxwell, L. D. van Buuren, and J. M. Doyle, Rev. Sci. Instrum. **75**, 17 (2004).
[19] J. G. E. Harris, Rev. Sci. Instrum. **79**, 030901 (2008).
[20] K. J. Matherson, R. D. Glover, D. E. Laban, and R. T. Sang, Rev. Sci. Instrum. **78**, 073102 (2007).
[21] K. J. Matherson, R. D. Glover, D. E. Laban, and R. T. Sang, Phys. Rev. A **78**, 042712 (2008).
[22] R. D. Glover, D. E. Laban, K. J. Matherson, W. Wallace, and R. T. Sang, J. Phys.: Conf. Ser. **212**, 012013 (2010).
[23] T. V. Tscherbul, Z. Pavlovic, H. R. Sadeghpour, R. Côté, and A. Dalgarno, Phys. Rev. A **82**, 022704 (2010).
[24] B. C. Sawyer, B. K. Stuhl, D. Wang, M. Yeo, and J. Ye, Phys. Rev. Lett. **101**, 203203 (2008).
[25] R. S. Schappe, T. Walker, L. W. Anderson, and C. C. Lin, Phys. Rev. Lett. **76**, 4328 (1996).
[26] P. Würtz, T. Gericke, A. Vogler, and H. Ott, New J. Phys. **12**, 065033 (2010).
[27] R. Schappe, M. Keeler, T. Zimmerman, M. Larsen, P. Feng, R. Nesnidal, J. Boffard, T. Walker, L. Anderson, and C. Lin, in *Methods of Measuring Electron-Atom Collision Cross Sections with an Atom Trap*, edited by B. Bederson and H. Walther, Vol. 48 of Advances in Atomic, Molecular, and Optical Physics (Academic Press, San Diego, 2002), pp. 357–390.
[28] J. Blieck, X. Fléchard, A. Cassimi, H. Gilles, S. Girard, and D. Hennecart, J. Phys.: Conference Series **163**, 012070 (2009).
[29] A. T. Grier, M. Cetina, F. Oručević, and V. Vuletić, Phys. Rev. Lett. **102**, 223201 (2009).
[30] C. Zipkes, S. Palzer, L. Ratschbacher, C. Sias, and M. Köhl, Phys. Rev. Lett. **105**, 133201 (2010).
[31] B. J. Claessens, J. P. Ashmore, R. T. Sang, W. R. MacGillivray, H. C. W. Beijerinck, and E. J. D. Vredenbregt, Phys. Rev. A **73**, 012706 (2006).
[32] K.-A. Brickman, M.-S. Chang, M. Acton, A. Chew, D. Matsukevich, P. C. Haljan, V. S. Bagnato, and C. Monroe, Phys. Rev. A **76**, 043411 (2007).
[33] D. N. Madsen and J. W. Thomsen, J. Phys. B **35**, 2173 (2002).
[34] D. E. Fagnan, J. Wang, C. Zhu, P. Djuricanin, B. G. Klappauf, J. L. Booth, and K. W. Madison, Phys. Rev. A **80**, 022712 (2009).
[35] T. Bergeman, G. Erez, and H. J. Metcalf, Phys. Rev. A **35**, 1535 (1987).
[36] K. B. Davis, M.-O. Mewes, M. A. Joffe, M. R. Andrews, and W. Ketterle, Phys. Rev. Lett. **74**, 5202 (1995).
[37] R. Wang, M. Liu, F. Minardi, and M. Kasevich, Phys. Rev. A **75**, 013610 (2007).
[38] A. M. Steane, M. Chowdhury, and C. J. Foot, J. Opt. Soc. Am. B **9**, 2142 (1992).
[39] J. Szczepkowski, E. Paul-Kwiek, G. Auböck, L. Holler, C. Binder, and L. Windholz, Eur. Phys. J. - Spec. Top. **144**, 265 (2007).
[40] E. L. Raab, M. Prentiss, A. Cable, S. Chu, and D. E. Pritchard, Phys. Rev. Lett. **59**, 2631 (1987).

[41] V. S. Bagnato, L. G. Marcassa, S. G. Miranda, S. R. Muniz, and A. L. de Oliveira, Phys. Rev. A **62**, 013404 (2000).
[42] D. Hoffmann, S. Bali, and T. Walker, Phys. Rev. A **54**, R1030 (1996).
[43] S. Friebel, C. D'Andrea, J. Walz, M. Weitz, and T. W. Hänsch, Phys. Rev. A **57**, R20 (1998).
[44] R. Jáuregui, N. Poli, G. Roati, and G. Modugno, Phys. Rev. A **64**, 033403 (2001).
[45] S. Balik, A. L. Win, and M. D. Havey, Phys. Rev. A **80**, 023404 (2009).
[46] J. Wu, R. Newell, M. Hausmann, D. J. Vieira, and X. Zhao, J. Appl. Phys. **100**, 054903 (2006).
[47] T. V. Tscherbul, P. Zhang, H. R. Sadeghpour, A. Dalgarno, N. Brahms, Y. S. Au, and J. M. Doyle, Phys. Rev. A **78**, 060703 (2008).
[48] T. V. Tscherbul, P. Zhang, H. R. Sadeghpour, and A. Dalgarno, Phys. Rev. A **79**, 062707 (2009).
[49] A. Dalgarno and W. Davison, Mol. Phys. **13**, 479 (1967).
[50] J. Mitroy and J.-Y. Zhang, Phys. Rev. A **76**, 032706 (2007).
[51] M. H. Shah, H. A. Camp, M. L. Trachy, G. Veshapidze, M. A. Gearba, and B. D. DePaola, Phys. Rev. A **75**, 053418 (2007).
[52] S. Bali, D. Hoffmann, and T. Walker, Europhys. Lett. **27**, 273 (1994).
[53] L. Landau and L. Lifshitz, *Quantum Mechanics, Non-relativistic Theory* (Pergamon, New York, 1965).
[54] M. Child, *Molecular Collision Theory* (Academic Press, New York, 1974).
[55] N. Marković, unpublished, Chalmers University of Technology, Göteborg, Sweden, 2003.
[56] B. Johnson, J. Comput. Phys. **13**, 445 (1973).
[57] B. Ueberholz, S. Kuhr, D. Frese, V. Gomer, and D. Meschede, J. Phys. B **35**, 4899 (2002).
[58] G. D. Telles, V. S. Bagnato, and L. G. Marcassa, Phys. Rev. Lett. **86**, 4496 (2001).
[59] J. L. Booth, J. Van Dongen, P. Lebel, B. G. Klappauf, and K. W. Madison, J. Opt. Soc. Am. B **24**, 2914 (2007).
[60] K. R. Overstreet, P. Zabawa, J. Tallant, A. Schwettmann, and J. P. Shaffer, Opt. Express **13**, 9672 (2005).
[61] T. P. Dinneen, K. R. Vogel, E. Arimondo, J. L. Hall, and A. Gallagher, Phys. Rev. A **59**, 1216 (1999).
[62] M. Prentiss, A. Cable, J. E. Bjorkholm, S. Chu, E. L. Raab, and D. E. Pritchard, Opt. Lett. **13**, 452 (1988).
[63] H. C. Busch, M. K. Shaffer, E. M. Ahmed, and C. I. Sukenik, Phys. Rev. A **73**, 023406 (2006).
[64] H. C. W. Beijerinck, Phys. Rev. A **62**, 063614 (2000).
[65] S. Rosin and I. I. Rabi, Phys. Rev. **48**, 373 (1935).
[66] G. Mahan, J. Chem. Phys. **48**, 950 (1968).
[67] D. Fagnan, honor's thesis, University of British Columbia, 2009.
[68] M. Movre and G. Pichler, J. Phys. B **10**, 2631 (1977).
[69] M. Movre and G. Pichler, J. Phys. B **13**, 697 (1980).
[70] A. Gallagher and D. E. Pritchard, Phys. Rev. Lett. **63**, 957 (1989).
[71] S. Bali, K. M. O'Hara, M. E. Gehm, S. R. Granade, and J. E. Thomas, Phys. Rev. A **60**, R29 (1999).